HIGH RESOLUTION VECTOR-SENSOR ARRAY PROCESSING USING QUATERNIONS

S. Miron, N. Le Bihan and J. I. Mars

Laboratoire des Images et des Signaux
961 rue de la Houille Blanche, BP. 46
38402 St. Martin d'Hères cedex, FRANCE

ABSTRACT

The aim of this paper is to introduce a novel MUSIC-like algorithm for polarized sources characterization based on a quaternion model for two-component sensor-array signal. The associated data covariance matrix is described and a comparison with the classical long-vector approach is made. We show that the use of quaternions improves the signal subspace estimation accuracy and reduces the computational burden. Additionally, the proposed algorithm presents a better resolution power for direction of arrival (DOA) estimation than the long-vector approach, for equivalent statistical performances.

1. INTRODUCTION

In the last few years, thanks to advances in sensor technology, vector-sensor[1] arrays were successfully used in various domains (communications, seismology, etc.), to improve sources characterization and discrimination. In order to extract information from the recorded datasets, algorithms for diversely polarized arrays were proposed by several authors ([1], [2]). An analysis of vector-sensor arrays performance was carried out in [3]. Most of the algorithms given in the literature are based on the long-vector technique, that is the concatenation of the components in a long-vector, allowing therefore the use of well established scalar-sensor array processing methods based on matrix algebra techniques.

In this paper we propose a quaternion model for a two-components (2C) vector-sensor array signals which uses more efficiently the multidimensional information. Quaternion - based techniques have already been proposed in signal processing by several authors (see [4, 5, 6] and references therein). In frequency domain, the data are complex-valued, representing the modulus and phase of the signals. The proposed model encodes the two complex-valued components of a polarized source recorded on a sensor-array in a vector of quaternions, allowing a compact handling of the multicomponent information. Consequently, a data covariance model is introduced as the quaternion spectral matrix (QSM) and a MUSIC-like algorithm for polarized sources characterization is proposed. We show that, thanks to a stronger orthogonality constraint, the new algorithm achieves a more accurate estimation of the signal subspace and a better DOA resolution compared with the long-vector approach. The use of quaternions also reduces the computational burden and the memory size required for computation.

[1] A vector-sensor (or multicomponent sensor) is a group of collocated (often mutually orthogonal) unidirectional scalar-sensors (usually two-2C or three-3C) allowing to record simultaneously the pulsation of a polarized wavefield in several space dimensions.

2. PROPOSED APPROACH

2.1. Quaternions

A quaternion is a four-dimensional hypercomplex number that can be written as:

$$q = q_0 + \mathtt{i}q_1 + \mathtt{j}q_2 + \mathtt{k}q_3, \tag{1}$$

where

$$\mathtt{i}^2 = \mathtt{j}^2 = \mathtt{k}^2 = \mathtt{ijk} = -1. \tag{2}$$

The conjugate of a quaternion is given by:

$$\bar{q} = q_0 - \mathtt{i}q_1 - \mathtt{j}q_2 - \mathtt{k}q_3, \tag{3}$$

and its modulus is:

$$|q| = \sqrt{q\overline{q}} = \sqrt{\overline{q}q} = \sqrt{q_0^2 + q_1^2 + q_2^2 + q_3^2}. \tag{4}$$

The set of quaternions, noted $\mathbb{H}$, forms a noncommutative algebra. In general, given two quaternions p and q, then

$$pq \neq qp \text{ and } \overline{pq} = \bar{q}\bar{p}. \tag{5}$$

A quaternion can be also expressed in the Cayley-Dickson form [7] as:

$$q = q^{(1)} + \mathtt{j}q^{(2)}, \tag{6}$$

where $q^{(1)} = q_0 + \mathtt{i}q_1$ and $q^{(2)} = q_2 - \mathtt{i}q_3$. A version of this notation is used in next subsection to model a two-component complex signal. A thorough review of quaternions can be found in [8]

2.2. Polarized signal model

Consider a 2C linear vector-sensor array formed of N equally-spaced sensors. In Fourier domain, at fixed frequency, observation on this array is given by two complex vectors $\mathbf{y}_1, \mathbf{y}_2 \in \mathbb{C}^N$, one for each component. Using an alternate form of Cayley-Dickson expression of a quaternion given in subsection (2.1), the following quaternion-valued vector $\mathbf{y} \in \mathbb{H}^N$ can be constructed:

$$\mathbf{y} = \mathbf{y}_1 + \mathtt{i}\mathbf{y}_2 \tag{7}$$

in which $\mathbf{y}_1$ and $\mathbf{y}_2$ are $\mathtt{j}$-complex vectors. When using the long-vector techniques, $\mathbf{y}_1, \mathbf{y}_2$ are concatenated forming the extended complex vector $\tilde{\mathbf{y}} \in \mathbb{C}^{2N}$, $\tilde{\mathbf{y}} = [\mathbf{y}_1^T | \mathbf{y}_2^T]^T$.

Consider now a scenario with F decorrelated sources impinging on the array. The sources are modeled by stationary stochastic processes and the propagation medium is supposed isotropic. Noise is spatially white and not polarized. If the sources are all confined in the array plane, their DOA is given by a single parameter. For simplicity, we consider that the location of a source f is specified by the inter-sensor phase-shift θ_f and its polarization is characterized by: the amplitude ratio between the components ρ_f and the intercomponent phase shift φ_f. Thus, the global behavior of the f^{th} source on the array is modeled by the quaternion vector $\mathbf{s}_f \in \mathbb{H}^N$:

$$\mathbf{s}_f(\theta_f, \rho_f, \varphi_f) = p_f(\rho_f, \varphi_f)\mathbf{a}_f(\theta_f), \tag{8}$$

where: $p_f(\rho_f, \varphi_f) = 1 + \mathtt{i}\rho_f e^{\mathtt{j}\varphi_f}$, and:

$$\mathbf{a}_f(\theta_f) = \left[1, e^{-\mathtt{j}\theta_f}, \ldots, e^{-\mathtt{j}(N-1)\theta_f}\right]^T. \tag{9}$$

Thus:

$$\mathbf{s}_f(\theta_f, \rho_f, \varphi_f) = \begin{bmatrix} 1 + \mathtt{i}\rho_f e^{\mathtt{j}\varphi_f} \\ e^{-\mathtt{j}\theta_f} + \mathtt{i}\rho_f e^{\mathtt{j}(\varphi_f - \theta_f)} \\ \vdots \\ e^{-\mathtt{j}(N-1)\theta_f} + \mathtt{i}\rho_f e^{\mathtt{j}(\varphi_f - (N-1)\theta_f)} \end{bmatrix}. \tag{10}$$

Consequently, the recorded signal on the antenna can be written as:

$$\mathbf{y} = \sum_{f=1}^{F} \mathbf{s}_f \sigma_f + \mathbf{n}, \tag{11}$$

where $\mathbf{n}$ is a quaternion vector containing noise contribution on the two components of the array and σ_f is the $\mathtt{j}$-complex amplitude of the source on the first component of the array.

2.3. Quaternion spectral matrix

An observation on the 2C antenna is given by a quaternion vector $\mathbf{y} \in \mathbb{H}^N$. The data covariance matrix associated to this model is the quaternion spectral matrix, $\mathbf{\Omega} \in \mathbb{H}^{N \times N}$:

$$\mathbf{\Omega} = \mathbb{E}[\mathbf{y}\mathbf{y}^\dagger], \tag{12}$$

where $\mathbb{E}[.]$ is the mathematical expectation operator and † represents the transposition-conjugation. Substituting (7) in (12), the representation of $\mathbf{\Omega}$ becomes:

$$\mathbf{\Omega} = \mathbb{E}[\mathbf{y}_1\mathbf{y}_1^\dagger] - \mathbb{E}[\mathbf{y}_1\mathbf{y}_2^\dagger]\mathtt{i} + \mathtt{i}\mathbb{E}[\mathbf{y}_2\mathbf{y}_1^\dagger] - \mathtt{i}\mathbb{E}[\mathbf{y}_2\mathbf{y}_2^\dagger]\mathtt{i}. \tag{13}$$

When considering (13) the reader must keep in mind that $\mathbf{y}_1, \mathbf{y}_2$ are $\mathtt{j}$-complex vectors and multiplication by $\mathtt{i}$ of a $\mathtt{j}$-complex number is not commutative. One can identify in (13) the expressions of auto-covariance and cross-covariance matrices for the two components of the vector array, meaning that QSM contains intrinsically all the second-order information available on the antenna.

Using (11) and the sources and noise decorrelation assumptions, the expression of the QSM becomes:

$$\mathbf{\Omega} = \sum_{f=1}^{F} \sigma_f^2 \mathbf{s}_f \mathbf{s}_f^\dagger + \mathbf{\Omega}_n, \tag{14}$$

where $\mathbf{\Omega}_n = \mathbb{E}[\mathbf{n}\mathbf{n}^\dagger]$ contains noise second order statistics and σ_f^2 represents the power of source f on the antenna.

The analogous covariance matrix for long-vector case, $\tilde{\mathbf{\Omega}} \in \mathbb{C}^{2N \times 2N}$ ($\tilde{\mathbf{\Omega}} = \mathbb{E}[\tilde{\mathbf{y}}\tilde{\mathbf{y}}^\dagger]$) contains $(2 \times N)^2 = 4 \times N^2$ complex entries, that is $8 \times N^2$ real fields while the quaternion spectral matrix in (12) has only $4 \times N^2$ real values, reducing by half the memory size required for computation. The computational burden for quaternion spectral matrix estimation is detailed in subsection 2.6.

2.4. Quaternion and complex orthogonality

In order to use subspace-based methods, the quaternion spectral matrix must be diagonalized by means of *Quaternion EigenValue Decomposition* [7]. As the existence of left eigenvalues of a quaternion matrix is problematic [9], the right quaternion eigenvalues and the right quaternion eigenvectors are considered in this paper. Quaternion spectral matrix can thus be written as:

$$\mathbf{\Omega} = \sum_{f=1}^{N} \lambda_f \mathbf{u}_f \mathbf{u}_f^\dagger, \tag{15}$$

where λ_f are the real eigenvalues (as $\mathbf{\Omega} = \mathbf{\Omega}^\dagger$) and $\mathbf{u}_f$ are the N orthonormal quaternion-valued eigenvectors. Two quaternion random vectors $\mathbf{p}, \mathbf{q} \in \mathbb{H}^N$ are *orthogonal* if:

$$< \mathbf{p}, \mathbf{q} >_{\mathbb{H}} = 0, \tag{16}$$

where $< \mathbf{p}, \mathbf{q} >_{\mathbb{H}} = \mathbb{E}[\mathbf{q}^\dagger \mathbf{p}]$ (see [10]).

Let us consider these two quaternion random vectors $\mathbf{p}, \mathbf{q}$ given as:

$$\mathbf{p} = \mathbf{p}_1 + \mathtt{i}\mathbf{p}_2 \ \text{ and } \ \mathbf{q} = \mathbf{q}_1 + \mathtt{i}\mathbf{q}_2 \tag{17}$$

and the associated long-vector forms $\tilde{\mathbf{p}}, \tilde{\mathbf{q}} \in \mathbb{C}^{2N}$:

$$\tilde{\mathbf{p}} = \left[\mathbf{p}_1^T | \mathbf{p}_2^T\right]^T \ \text{ and } \ \tilde{\mathbf{q}} = \left[\mathbf{q}_1^T | \mathbf{q}_2^T\right]^T \tag{18}$$

By imposing orthogonality between quaternion vectors $\mathbf{p}$ and $\mathbf{q}$ ($< \mathbf{p}, \mathbf{q} >_{\mathbb{H}} = 0$), the following relations are obtained:

$$< \mathbf{p}_1, \mathbf{q}_1 >_{\mathbb{C}} + < \mathbf{p}_2, \mathbf{q}_2 >_{\mathbb{C}} = 0 \tag{19}$$

and

$$< \mathbf{p}_2, \mathbf{q}_1^* >_{\mathbb{C}} = < \mathbf{p}_1, \mathbf{q}_2^* >_{\mathbb{C}}, \tag{20}$$

while the orthogonality condition[2] for the long-vector approach leads only to (19). This means that the quaternion vector orthogonality constraint imposed when diagonalizing QSM, is more restrictive in the choice of the eigenvectors than the long-vector orthogonality constraint.

To see how this stronger orthogonality constraint affects the subspace estimation in eigenstructure-based algorithms, two randomly-generated matrices $\mathbf{W}_1, \mathbf{W}_2 \in \mathbb{C}^{50\times 50}$ are considered. Assimilating these matrices to data recorded on a 2C sensor array, a quaternion matrix $\mathbf{W}_Q \in \mathbb{H}^{50\times 50}$ and a long-vector one $\mathbf{W}_{LV} \in \mathbb{C}^{100\times 50}$ are constructed as:

$$\mathbf{W}_Q = \mathbf{W}_1 + \mathtt{i}\mathbf{W}_2 \ \text{ and } \ \mathbf{W}_{LV} = \left[\mathbf{W}_1 | \mathbf{W}_2\right]^T. \tag{21}$$

Diagonalization and rank-R truncation ($0 < R < 50$) of $\mathbf{W}_Q$ and $\mathbf{W}_{LV}$ give $\mathbf{W}_Q^R$ and $\mathbf{W}_{LV}^R$ respectively (see [6]). Then:

$$err_Q(R) = \frac{\|\mathbf{W}_Q - \mathbf{W}_Q^R\|}{\|\mathbf{W}_Q\|} \tag{22}$$

and

$$err_{LV}(R) = \frac{\|\mathbf{W}_{LV} - \mathbf{W}_{LV}^R\|}{\|\mathbf{W}_{LV}\|} \tag{23}$$

give the normalized rank-R approximation error of $\mathbf{W}_Q$ and $\mathbf{W}_{LV}$, where $\|.\|$ designates the Frobenius norm.

In **Fig. 1**, $err_Q(R)$ and $err_{LV}(R)$ (in dB) are presented as functions of the rank-R approximation. Averaging over 100 independent realizations of $\mathbf{W}_1$ and $\mathbf{W}_2$ was performed. The quaternion approach concentrates the energy of the two-component dataset on the first eigenvectors better than the long-vector technique, as one can see in **Fig.1**. This means that on 2C recorded datasets, the energy of the signals is more accurately concentrated on signal subspace using quaternions than with the long-vector methods. This property is exploited in the following quaternion high resolution algorithm.

[2]Two complex random vectors $\tilde{\mathbf{p}}, \tilde{\mathbf{q}} \in \mathbb{C}^N$ are *orthogonal* if $< \tilde{\mathbf{p}}, \tilde{\mathbf{q}} >_{\mathbb{C}} = 0$, where $< \tilde{\mathbf{p}}, \tilde{\mathbf{q}} >_{\mathbb{C}} = \mathbb{E}[\tilde{\mathbf{q}}^\dagger \tilde{\mathbf{p}}]$.

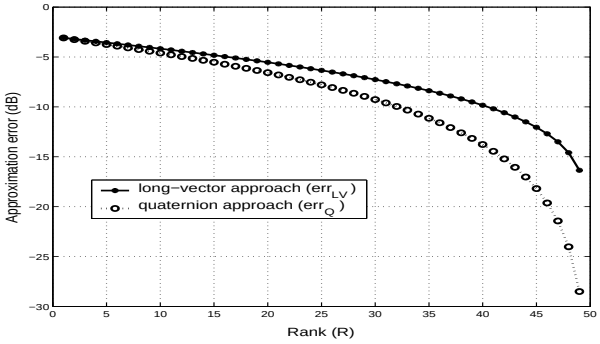

Fig. 1. Rank approximation error (in dB) for the quaternion and long-vector approaches

2.5. Quaternion-MUSIC

MUSIC-like methods are based on the projection of a steering vector on the estimated noise subspace. By identification of (14) with (15), we associate the first F eigenvalues to the signal part of the observation and the rest of $N-F$ to the noise part. Thus, the quaternion projector on the noise subspace is defined as:

$$\mathbf{\Pi}_n = \sum_{f=F+1}^{N} \mathbf{u}_f \mathbf{u}_f^\dagger. \tag{24}$$

An unitary quaternion steering-vector $\mathbf{q}(\theta, \rho, \varphi) \in \mathbb{H}^N$, modeling the arrival of a polarized source on the antenna is then generated dividing

$$\mathbf{q}(\theta, \rho, \varphi) = \begin{pmatrix} 1 + \mathtt{i}\rho \mathrm{e}^{\mathtt{j}\varphi} \\ \mathrm{e}^{-\mathtt{j}\theta} + \mathtt{i}\rho \mathrm{e}^{\mathtt{j}(\varphi-\theta)} \\ \vdots \\ \mathrm{e}^{-\mathtt{j}(N-1)\theta} + \mathtt{i}\rho \mathrm{e}^{\mathtt{j}(\varphi-(N-1)\theta)} \end{pmatrix} \tag{25}$$

by its norm. The Quaternion-MUSIC estimator (Q-MUSIC) depending on three parameters is computed by projecting $\mathbf{q}$ on the noise subspace:

$$\mathcal{Q}(\theta, \rho, \varphi) = \frac{1}{\mathbf{q}^\dagger(\theta, \rho, \varphi) \mathbf{\Pi}_n \mathbf{q}(\theta, \rho, \varphi)} \tag{26}$$

The function in (26) has maxima for sets of (θ, ρ, φ) corresponding to sources present in the signal. By varying θ, ρ, φ within a given domain with a chosen step, a three dimensional surface is computed. The estimated values of θ, ρ and φ are the coordinates of the most important local maxima on this surface. Assuming that the iteration step is sufficiently small for a correct sampling of the hyper-surface, the search for local maxima is automatically done by comparing each point on this surface with its neighbors. The first F maxima correspond to the F sources present in the signal. This way, the estimation process of θ, ρ and φ is quasi-unsupervised.

2.6. Computational issues

This section addresses the problem of computational complexity for long-vector and quaternion algorithms. A full estimation of the computational complexity of the methods is difficult and is little relevant as it is hardware and software dependent. In the sequel we only focus on one aspect of the algorithm: the estimation of the covariance matrix. This procedure, as it implies repetitive operations, best illustrates the complexity differences between the two algorithms. The complexity of the methods are evaluated in terms of memory requirements, memory traffic and basic arithmetical operations: real numbers addition (A), multiplication (M) and division (D).

Let us consider a vector-sensor array composed of N two-component sensors. In frequency domain, a snapshot of the array is given by two complex-valued vectors $\mathbf{p}_1, \mathbf{p}_2 \in \mathbb{C}^N$. The quaternion representation $\mathbf{p} \in \mathbb{H}^N$ and the long-vector representation $\tilde{\mathbf{p}} \in \mathbb{C}^{2N}$ of the observation vector have the expressions given by (17) and (18). The corresponding covariance matrices are as it follows:

$$\mathbf{\Omega} = \mathbb{E}[\mathbf{p}\mathbf{p}^\dagger] \in \mathbb{H}^{N\times N} \text{ and } \tilde{\mathbf{\Omega}} = \mathbb{E}[\tilde{\mathbf{p}}\tilde{\mathbf{p}}^\dagger] \in \mathbb{C}^{2N\times 2N}. \tag{27}$$

If averaging over L particular realizations of the covariance matrix is used for estimation, we can write:

$$\mathbf{\Omega} = \frac{1}{L}\sum_{l=1}^{L} \mathbf{p}_l\mathbf{p}_l^\dagger = \frac{1}{L}\sum_{l=1}^{L} \mathbf{\Omega}_l \tag{28}$$

and

$$\tilde{\mathbf{\Omega}} = \frac{1}{L}\sum_{l=1}^{L} \tilde{\mathbf{p}}_l\tilde{\mathbf{p}}_l^\dagger = \frac{1}{L}\sum_{l=1}^{L} \tilde{\mathbf{\Omega}}_l. \tag{29}$$

Each one of the $\mathbf{\Omega}_l$ matrices has N^2 quaternionic entries and can be represented at machine memory level on $4N^2$ real fields, while the $\tilde{\mathbf{\Omega}}_l$ matrices have $4N^2$ complex entries each, corresponding to $8N^2$ real values. This way, quaternion algorithm reduces by half the memory requirements for representation of data covariance model, resulting also in a total diminution by a factor of ≈ 2 of memory traffic operations (data retrieving and writing) and a proportional speed gain.

Let us evaluate now the total number of basic arithmetical operations needed to estimate the covariance matrix. Each of the quaternion entries of $\mathbf{\Omega}_l$ is the result of the multiplication of two quaternions. Multiplication of two quaternions implies 16 real multiplications (M) and 12 real additions (A), that is a total of $16N^2$ (M) and $12N^2$ (A) for the whole matrix. For the complex matrix $\tilde{\mathbf{\Omega}}_l$ we have $16N^2$ (M) and $8N^2$ (A).

Thus, the summation $\sum_{l=1}^{L} \mathbf{\Omega}_l$ needs a total of $16N^2L$ (M) and $12N^2L + (L-1)4N^2 = 16N^2L - 4N^2$ (A) while $\sum_{l=1}^{L} \tilde{\mathbf{\Omega}}_l$ requires $16N^2L$ (M) and $8N^2L + (L-1)8N^2 = 16N^2L - 8N^2$(A). These results take into account the observation vectors multiplication as well as matrices addition. The final division by L means another $4N^2$ real numbers divisions (D) for the quaternion algorithm and $8N^2$ (D) for the long-vector one. **Table 1** recapitulates the covariance matrix computational effort for the two algorithms.

As we can see, the quaternion algorithm reduces the memory requirements for data covariance model representation by a factor of two. Consequently, the memory traffic is reduced by approximately the same factor, resulting in an important gain in rapidity, especially for large data size. Regarding the number of elementary operations on real values, the quaternionic approach demands $4N^2$ additions moreover and $4N^2$ divisions less than the long-vector method. The computational complexity for division is several times more important than for addition, implying higher computational cost for long-vector.

The computation of the quaternionic eigenvectors of the estimated matrix $\mathbf{\Omega} \in \mathbb{H}^{N\times N}$ can be performed using algorithms dealing with complex numbers or quaternions. The methods based on complex numbers come down to diagonalizing the complex adjoint matrix of $\mathbf{\Omega}$, that is a complex-valued matrix of size $2N \times 2N$ (see [7, 11]). In this case, the computational complexity of the eigenvalue decomposition of the quaternionic matrix $\mathbf{\Omega}$ is equivalent to the decomposition complexity of the complex matrix $\tilde{\mathbf{\Omega}}$. The advantage of this approach is given by the possibility of using complex matrix diagonalization routines already existing in the literature (ex. LAPACK), that are computationally optimized.

Nevertheless, it was shown (see [12]) that working directly in quaternionic domain improves the convergence speed of the algorithms compared to complex approach. This reinforces the idea that the use of quaternions can enhance the performance of algorithms.

Generally, the use of quaternions in algorithms reduces the computational effort, due to the compact handling of the data.

3. RESULTS

In this section, a comparison between the Q-MUSIC and the long-vector MUSIC algorithm is presented for different source configurations. First, a polarized source impinging on an array of 20 two-component sensors is considered. The simulated parameters for the source are $\theta = 0.44\ rad, \rho = 1, \varphi = -30^o$. In **Fig. 2** we plotted the DOA curve for the quaternion and the long-vector approach, assuming the polarization parameters known. Five hundred trials have been used to estimate the covariance matrices. As we can note in **Fig. 2**, the two detection curves for the algorithms are almost completely superposed. However, the quaternion algorithm seems to be slightly more resolutive (the amplitude of the detection lobe is more important) than the long-vector

	Memory requirements $(real\ values)$	Memory operations	Real multiplications (M)	Real additions (A)	Real divisions (D)
quaternion SM	$4N^2$	$\approx 4N^2L$	$16N^2L$	$16N^2L - 4N^2$	$4N^2$
long-vector SM	$8N^2$	$\approx 8N^2L$	$16N^2L$	$16N^2L - 8N^2$	$8N^2$

Table 1. Computational effort for covariance matrix estimation

one. The explanation to this result is the stronger orthogonality constraint (described in subsection 2.4) imposed by the quaternion approach.

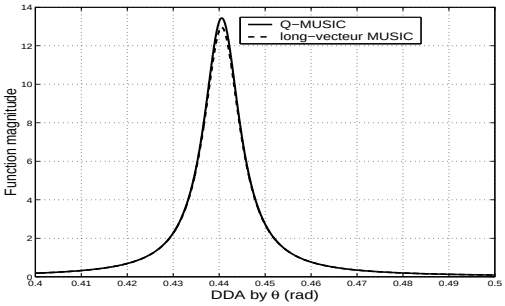

Fig. 2. DOA estimation for one source
Cut for $\rho_1 = 1\ (rad)$ and $\varphi_1 = -30^o$ $(\mathbf{s}_1)$

A scenario with three differently polarized sources is then considered. The simulated parameters for the sources are given in **Table 2**. **Fig. 3** ((a) and (b)) shows the polarization plane for the DOA $\theta_1 = -1$ corresponding to the first source.

	$\mathbf{s}_1$	$\mathbf{s}_2$	$\mathbf{s}_3$
θ (rad)	0.44	-0.44	-0.88
ρ	1	3	5
φ (degrees)	-30	-10	20

Table 2. Simulated parameters for the three sources

When using Q-MUSIC, the estimated values for the polarization parameters are $\widehat{\rho}_1^Q = 1.15$ and $\widehat{\varphi}_1^Q = -28^o$, whereas for the long-vector algorithm the estimated parameters are $\widehat{\rho}_1^{LV} = 1.2$, $\widehat{\varphi}_1^{LV} = -27^o$. The polarization path (the detection cone) is wider for Q-MUSIC, meaning that the proposed method is less resolutive in polarization parameters plane. This is a direct consequence of memory requirements reduction for QSM computation (see subsection 2.6). The multicomponent (polarization) dimension of the data is compressed when computing QSM, resulting in a less accurate separation of sources in polarization domain. This fact is also illustrated in **Fig. 4** that plots DOA curves corresponding to polarization parameters of the first source, for both algorithms. We see that for Q-MUSIC, the other two sources ($\mathbf{s}_2$ et $\mathbf{s}_3$) are still present on the detection curve

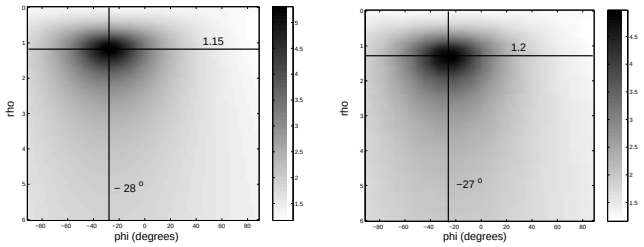

(a) Q-MUSIC (b) long-vector MUSIC

Fig. 3. Polarization estimation for the first source
Cut for $\theta_1 = 0.44\ (rad)$ $(\mathbf{s}_1)$

corresponding to first source polarization parameters. The

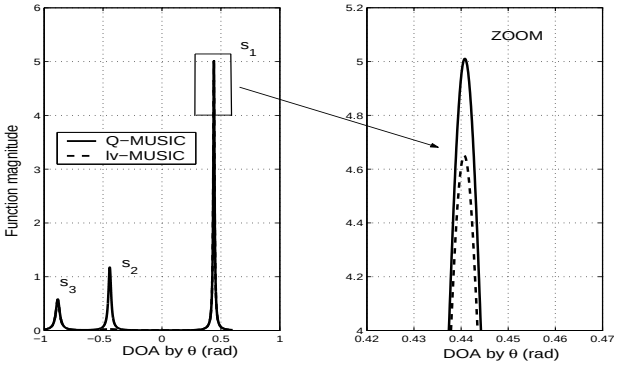

Fig. 4. DOA estimation for three sources
Cut for $\rho_1 = 1\ (rad)$ and $\varphi_1 = -30^o$ $(\mathbf{s}_1)$

right side of **Fig. 4** represents a zoom of the detection peak for $\mathbf{s}_1$, showing that, even in a multiple source scenario, the quaternion approach presents a stronger answer for sources DOA estimation.

In order to have a statistical characterization of Q-MUSIC estimator, its performance is compared to long-vector MUSIC and classical MUSIC (for scalar arrays) in Monte Carlo runs. Consider two equal-power uncorrelated polarized sources, with random initial phases, impinging on a two-component sensor-array composed of 10 equally-spaced sensors. The sources DOAs are $\theta_1 = -0.7\ rad$, $\theta_2 = 0.5\ rad$ and they have the following polarization parameters: $\rho_1 = 2.5$, $\varphi_1 = -0.18\ rad$, $\rho_2 = 3$, $\varphi_2 = 0.15\ rad$. Figure 5 plots the DOA root-mean-square (RMS) estimation error for the estimators mentioned bellow. One hundred snapshots are

used in each Monte Carlo run. Three hundred independent runs contribute to each number in the figure. Additive white gaussian noise is present in different signal to noise proportions. The RMS error for DOA estimation is defined as the root-mean-square of the RMS estimation error of θ_1 and θ_2:

$$RMS(\widehat{\theta}) = \sqrt{\frac{RMS^2(\widehat{\theta_1}) + RMS^2(\widehat{\theta_2})}{2}}.$$

For Scalar-MUSIC a mean is operated over the two components. Fig 5 shows that the two algorithms, Q-MUSIC and long-vector MUSIC, present equivalent performance, their RMS error curves are almost totally superposed. Nevertheless, their estimation error is clearly inferior to scalar version of the algorithm.

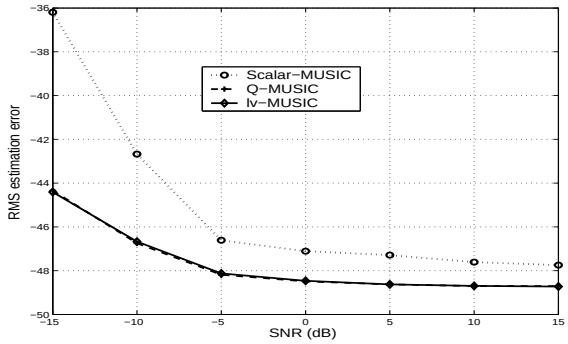

Fig. 5. RMS estimation error (dB) for DOA versus SNR (dB)

4. CONCLUSIONS

This paper illustrates the potentiality of hypercomplex numbers in statistical signal processing.

We have proposed an eigenstructure-based algorithm for multiple sources characterization on a 2C-sensor array based on a novel quaternion model for 2C complex-valued dataset. Q-MUSIC proved to be more sensitive to sources DOAs than the classical long-vector version, for equivalent statistical performance. We showed that a more accurate estimation of the signal subspace is achieved provided that hypercomplex algebra is used. The memory requirement for covariance matrix computation are diminished by half, resulting in a proportional reduction of computational burden. However, the proposed method is less sensitive to polarization parameters estimation compared to long-vector approach. Nevertheless, quaternion formalism provides an elegant and compact way of handling multicomponent data.

5. REFERENCES

[1] J. Li and Jr. R.T. Compton, "Angle and polarization estimation using ESPRIT with a polarization sensitive array," *IEEE Trans. Antennas Propagat.*, vol. 39, no. 9, pp. 1376–1383, Sept. 1991.

[2] K. T. Wong and M. D. Zoltowski, "Diversely polarized root-MUSIC for azimuth-elevation angle of arrival estimation," in *Digest of the 1996 IEEE Antennas Propagation Soc. Int. Symp.*, Baltimore, July 1996, pp. 1352–1355.

[3] A. J. Weiss and B. Friedlander, "Performance analysis of diversly polarized antenne arrays," *IEEE Trans. Signal Processing*, vol. 39, no. 7, pp. 1589–1603, July 1991.

[4] S. C. Pei and C. M. Cheng, "A novel block truncation coding of color images using a quaternion-moment-preserving principle," *IEEE Trans. Communications and Systems*, vol. 45, no. 5, pp. 583–595, May 1997.

[5] S. J. Sangwine and T. A. Ell, "Hypercomplex auto- and cross-correlation of color images," *IEEE International Conference on Image Processing (ICIP), Kobe, Japan*, pp. 319–322, 1999.

[6] N. Le Bihan and J. Mars, "Singular value decomposition of matrices of quaternions: A new tool for vector-sensor signal processing," *Signal Processing*, vol. 84, no. 7, pp. 1177–1199, 2004.

[7] H. C. Lee, "Eigenvalues and canonical forms of matrices with quaternion coefficients," in *Proc. of the Royal Irish Academy*, Dec. 1949, vol. 52, pp. 253–261.

[8] J. P. Ward, *Quaternions and Cayley Numbers, Algebra and applications*, Kluwer Academic, 1997.

[9] L. Huang and W. So, "On left eigenvalues of a quaternionic matrix," *Linear Algebra and its Applications*, vol. 323, pp. 105–116, 2001.

[10] N. N. Vakhania, "Random vectors with values in quaternion Hilbert spaces," *Th. Probab. Appl.*, vol. 43, no. 1, pp. 99–115, 1998.

[11] R. M. W. Wood, "Quaternionic eigenvalues," *Bull. London Math. Soc.*, vol. 17, pp. 137–138, 1985.

[12] A. Bunse-Gerstner, R. Byers, and V. Mehrmann, "A quaternion QR algorithm," *Numerische Mathematik*, vol. 55, pp. 83–95, 1989.